

Atomic Correlation Between Adjacent Graphene Layers in Double-Wall Carbon Nanotubes

Ayako Hashimoto,^{1,*} Kazu Suenaga,¹ Koki Urita,^{1,2} Takashi Shimada,³ Toshiki Sugai,³ Shunji Bandow,⁴
Hisanori Shinohara,³ and Sumio Iijima^{1,4}

¹Research Center for Advanced Carbon Materials, National Institute of Advanced Industrial Science and Technology, Tsukuba, 305-8565, Japan

²Graduate School of Science and Technology, Chiba University, Chiba, 263-8522, Japan

³Department of Chemistry and Institute for Advanced Research, Nagoya University, Nagoya, 464-8602, Japan

⁴Department of Materials Science and Engineering, Meijo University, Nagoya, 468-8502, Japan

(Received 9 July 2004; published 3 February 2005)

Atomic correlation between adjacent graphene layers was elucidated for double-wall carbon nanotubes (DWNTs) through a chiral index assignment of two nested nanotubes by high-resolution transmission electron microscopy. Our analysis provides a rather constant diameter difference close to 0.75 nm but no chiral angle correlation between the constituent nanotubes in the concentric DWNTs. The local atomic correlation as a commensurate graphene stacking was repeatedly found in eccentric DWNTs and circumscribed nanotubes, which should lead to elastic deformation and bundling of nanotubes.

DOI: 10.1103/PhysRevLett.94.045504

PACS numbers: 61.46.+w, 68.37.Lp, 81.05.Uw

Interaction between two adjacent graphene layers often governs the structures and properties of nanocarbon materials. It is well known that the interlayer distance between two flat graphene layers ranges from 0.34 nm for highly oriented pyrolytic graphite (HOPG) to 0.35 nm for turbostratic graphite, depending on the atomic correlation between the adjacent layers with the van der Waals interaction. While the electronic property of a single-wall carbon nanotube (SWNT) is determined by the lattice orientation of a rolled graphene layer, more intriguing properties are expected to occur in a multiwall carbon nanotube (MWNT) comprising nested SWNTs due to the interlayer interaction. Theoretical calculations for energy bands of MWNTs have concluded that the transport property of nested nanotubes was sensitive to the structural symmetry, that is, the atomic correlation between adjacent nanotubes [1–3]. It is therefore of prime importance to investigate such interlayer interaction before realizing the nanotube-based electronic devices. Nevertheless, the interaction has never been experimentally elucidated so far because it has been extremely difficult to explore the atomic correlation taking into account the subtle competition between the van der Waals interaction and the elastic force of a graphene layer.

In this study, the atomic correlations between the adjacent graphene layers have been experimentally clarified for different types of DWNTs, consisting of two nested nanotubes, through the chiral index determination by high-resolution transmission electron microscopy (HR-TEM) imaging. Raman spectroscopy [4] and x-ray diffraction studies [5], which have been often used for chirality analysis, are unable to investigate any chirality relationship for an individual DWNT but provide only the average values for the macroscopic amount of DWNTs. Electron diffraction could allow us to examine the chirality individually [6,7], but any local atomic correlation cannot be clarified

by the technique. On the other hand, the HR-TEM imaging used in our study is a novel way to reveal the local correlation of graphene layers.

The DWNTs prepared by two methods were investigated in this work. One was the peapod-derived DWNTs, which were produced by annealing SWNTs encapsulating C₆₀ molecules (denoted as A-DWNTs) [8], and the other was synthesized by a high-temperature pulsed arc discharge with Y/Ni doped electrodes (denoted as B-DWNTs) [9]. These DWNTs were observed by a conventional HR-TEM (JEOL, JEM-2010F) operated at 120 kV under our favorable conditions to visualize graphitic networks [10].

To identify two independent chiral indices of an individual DWNT accurately, the diameter (D) and chiral angle (α) were precisely measured for each constituent tube as described in the following. First, the “apparent” chiral angles can be estimated from a fast Fourier transform (FFT) of a HR-TEM image of the nanotubes. Figures 1(a)–1(c) show HR-TEM images of A-DWNT. The partial DWNT (bottom part) and the remaining SWNT (upper part) are characteristic to this specimen due to its growth process [8]. As seen in Fig. 1(b) upper, a moiré pattern at the SWNT part can be decomposed into a set of two hexagons in the FFT pattern. Then the apparent α can be obtained by measuring an angle of hexagonal spots to the tube axis, which corresponds to the lattice orientation of graphene layer. Similarly, two sets of hexagons can be assigned in the FFT of DWNT part [Fig. 1(c) upper], and then the apparent α of the inner nanotube can be extracted from the hexagonal spots which are missing at the SWNT part. The inverse FFT of the corresponding hexagonal spots selectively generates the zigzag lattice images either of the outer [Fig. 1(b) bottom] or the inner nanotubes [Fig. 1(c) bottom]. It should be noted that the measured apparent α may provide a considerable differ-

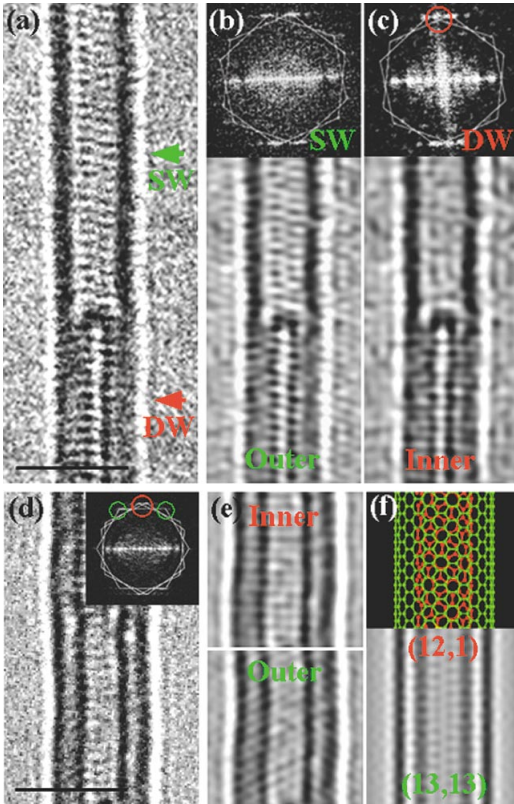


FIG. 1 (color). (a) A HR-TEM image of an A-DWNT, which has the partial DWNT (bottom) and the remaining SWNT (upper) parts. (b)–(c) (upper) FFT patterns of the SWNT (b) and DWNT (c) parts in the HR-TEM image. The additional spots (indicated by the red circle) are originating from the inner nanotube. (bottom) Inverse FFT images of the corresponding hexagonal spots, which selectively generate the zigzag lattice images either of the outer (b) and inner (c) nanotubes. (d) A HR-TEM image and FFT pattern of a B-DWNT. (e) Inverse FFT images of the inner (upper) and outer (bottom) nanotubes. (f) An atomic model (upper) and its simulated image (bottom) of the B-DWNT with the finalized chiral index pair [(12, 1) and (13, 13)]. Scale bars in all figures are 2 nm.

ence from the “true” α because of the high curvature of graphene layers [11], which must be adjusted later.

Second, we performed a systematic image simulation with our experimental TEM conditions in order to obtain the “true” diameters of examined SWNT [10,12] and DWNT. A simple measurement of the distance between paired dark lines (corresponding to the tube walls) exhibits a systematic and substantial deviation from the true D , even for a SWNT, due to the inevitable Fresnel fringes arising at the edges of the nanotubes. From the systematic simulation, we know that the “apparent” D is definitively smaller (~ 0.1 nm) than the true D in the case of SWNTs (the experimental conditions must be considered) [10]. It is more complicated to measure the two diameters of the constituent tubes in a DWNT because of the more intense interference of Fresnel fringes arising between two adjacent tube walls. The interspace between two walls tends to appear brighter due to the interference and the interlayer

distance is likely to be overestimated. Therefore, we made a multistep process: (i) a systematic image simulation of DWNTs with two variable diameters has been performed for the wide range of diameters with 0.01 nm step, (ii) the measured apparent D can be converted to the “approximately true” D with an error of ~ 0.05 nm by compensating the diameter, (iii) using these two “approximately true” D and apparent α , several solutions for a set of chiral indices of DWNTs can be obtained by following the Kociak’s table [6], and (iv) iterative image simulations are performed for several solutions to achieve the final set of chiral indices with the minimum errors. It is relatively easier to obtain a unique chiral index solution for a smaller nanotube because the smaller one has only a few possible solutions due to a specific diameter even though the FFT diffraction spots appear more diffused than those of the larger one. Figures 1(d)–1(f) show an example for the B-DWNT with the finalized chiral indices [the inner (13, 13) and outer (12, 1) nanotubes].

The obtained chiral indices for the both types of DWNTs are summarized in Table I including the D and α of both inner and outer nanotubes. The average outer tube diameter of B-DWNTs (~ 1.8 nm) is larger than that of A-DWNTs (~ 1.5 nm). To clarify any correlations between the two nested tubes, the chiral angle difference ($\Delta\alpha$) and the diameter difference $\Delta D(D_{\text{out}} - D_{\text{in}})$ are also presented for all the DWNTs. The two possible values for the $\Delta\alpha$ ($|\alpha_{\text{in}} - \alpha_{\text{out}}|$ and $|60 - \alpha_{\text{in}} + \alpha_{\text{out}}|$) are due to the optical inverse problem; i.e., right and left screws cannot be distinguished by the present HR-TEM. The result shows no significant correlation and no tendency in the chiral indices between the inner and outer nanotubes in both DWNTs. The $\Delta\alpha$ value is widely scattered between 0 and 60° . This is suggestive of the turbostratic stacking, indicating that the adjacent graphene layers of the both DWNTs exhibit no preferable orientational relationship. On the other hand, the ΔD of A- and B-DWNTs, which is related to the interlayer distance, are 0.73 ± 0.04 and 0.76 ± 0.07 nm, respectively. The average ΔD of B-DWNTs seems slightly larger than that of A-DWNTs and the constitute tubes in B-DWNTs sometimes shows collapsed defects. These differences between A- and B-DWNTs might originate from their synthesis routes. The average interlayer distance of both DWNTs ($\Delta D/2$) is obviously larger than that of HOPG (~ 0.34 nm). This large gap is most probably attributed to the turbostratic stacking and high curvature of graphene layers in nanotubes. For the observed DWNTs, we have assumed the two nested tubes are concentric, involving a uniform interlayer space between the inner and outer nanotubes along the tube axis.

In addition to the above concentric DWNTs, some peculiar DWNTs with an eccentric nested structure have been occasionally found for both DWNTs. In these DWNTs, the ΔD is quite large (more than 1 nm) and the inner nanotube is no longer positioned at the center of the outer one but keeping closer to one side of the outer tube wall. Figure 2(a) shows a HR-TEM image of a

TABLE I. Summary of the determined best fit chiral indices, α_{true} , D_{true} , calculated $\Delta\alpha$, and ΔD of inner and outer nanotubes in examined A- and B-DWNTs.

DWNT	Chiral Index (outer/inner tube)	α_{true} (deg) (outer/inner)	D_{true} (nm) (outer/inner)	$\Delta\alpha$ (deg)	ΔD (nm)
A1	(15, 3)/(8, 0)	8.9/0.0	1.31/0.63	8.9, 51.1	0.68
A2	(14, 5)/(6, 3)	14.7/19.1	1.34/0.62	4.4, 26.2	0.72
A3	(18, 4)/(7, 6)	9.8/27.5	1.59/0.88	17.7, 22.7	0.71
A4	(15, 5)/(8, 0)	13.9/0.0	1.41/0.63	13.9, 46.1	0.78
A5	(17, 6)/(7, 5)	14.6/27.0	1.62/0.82	12.4, 18.4	0.80
A6	(21, 6)/(10, 8)	12.2/26.3	1.92/1.22	14.1, 21.5	0.70
B1	(13, 13)/(12, 1)	30.0/4.0	1.76/0.98	26	0.78
B2	(15, 13)/(13, 2)	27.6/7.1	1.90/1.10	20.5, 25.3	0.80
B3	(20, 5)/(9, 7)	10.9/25.9	1.79/1.09	15.0, 23.2	0.70
B4	(21, 5)/(10, 6)	10.4/21.8	1.87/1.10	11.4, 27.8	0.77
B5	(23, 3)/(8, 7)	6.1/27.8	1.93/1.02	21.7, 26.1	0.91
B6	(17, 8)/(8, 7)	18.3/27.8	1.73/1.02	9.5, 13.9	0.71
B7	(22, 2)/(13, 1)	4.3/3.7	1.81/1.06	0.6, 52.0	0.75
B8	(15, 11)/(12, 3)	24.9/10.9	1.77/1.08	14.0, 24.2	0.69

peculiar A-DWNT. At the region marked by a red rectangle, the periodic lattice fringes are obviously linked through the two nanotube walls, indicating a local commensurate stacking between adjacent graphene layers. Since the lattice fringes correspond to the zigzag chain spacing of a graphene layer, it is suggestive that the zigzag chains tend to align between the adjacent layers. In another peculiar B-DWNT [Fig. 2(b)], a smaller (0.39 nm) inter-layer space with the commensurate lattice (a red rectangle) as well as a larger (0.54 nm) space (a green one) can be observed. An important issue derived from the result is that the large outer nanotube can elastically deform to provide a local atomic correlation (the red rectangle). This clearly reveals that a stronger van der Waals interaction with the

commensurate zigzag chains can sometimes overwhelm the elastic force of a graphene layer and lead to a deformation.

Such a local atomic correlation between two adjacent layers can be also seen in the neighboring two DWNTs. As

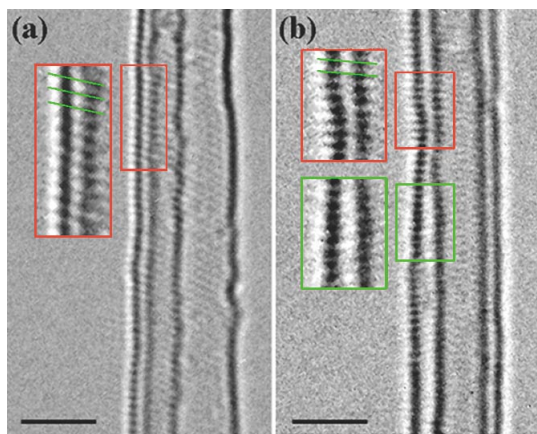


FIG. 2 (color). (a) A HR-TEM image of a peculiar A-DWNT with an eccentric nested structure. At the red-marked region, the lattice fringes are obviously linked through the two walls, indicating a local commensurate stacking. (b) A HR-TEM image of an eccentric B-DWNT. A smaller interlayer space with the commensurate lattice (a red rectangle) as well as a larger space (a green one) can be observed.

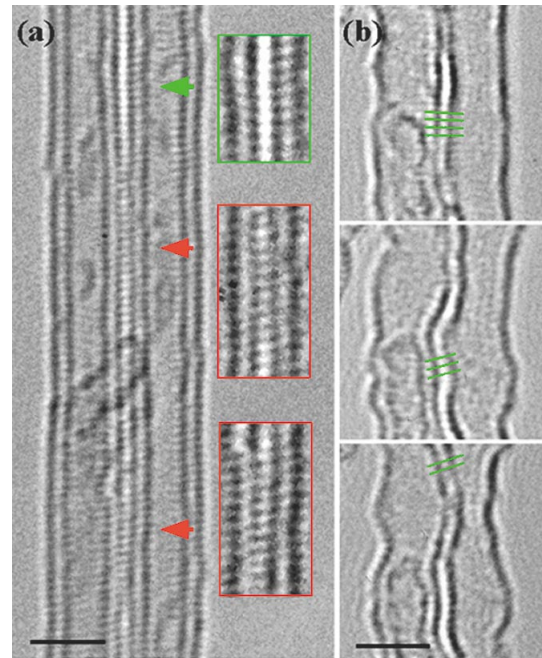


FIG. 3 (color). (a) A HR-TEM image of neighboring two DWNTs, in which red and green arrows highlight the commensurate and incommensurate stacking regions, respectively. (b) Structural changes of two circumscribed SWNTs under electron irradiation. (top) Initially, two nanotubes are parallel each other with the local atomic correlation indicated by green lines. (center and bottom) The circumscribed nanotubes exhibit a synchronized deformation in keeping a particular intertube distance.

shown in Fig. 3(a), the intertube distance shows a slight variation along the tube axis and similar local commensurate stacking of zigzag chains (highlighted by red arrows) is found from place to place between the two circumscribed outertubes. The green arrow shows an incommensurate region. This local correlation with the stronger van der Waals force should result in the tendency for neighboring carbon nanotubes to make a bundle (mainly for SWNTs), and lead to bend and sometimes twist the nanotubes. Figures 3(b) show structural changes of two circumscribed SWNTs during electron irradiation. Initially two nanotubes are parallel to each other with the local atomic correlation indicated by the partial linked lattice fringes [green lines in Fig. 3(b) top]. The two SWNTs show a strong curving or a local necking during the irradiation as shown in a sequence of images in Figs. 3(b) (center and bottom). Importantly, the two circumscribed walls exhibit the synchronized deformation in keeping a particular intertube distance (0.36 ~ 0.40 nm). The interaction exerted between the adjacent layers is strong enough to induce an elastic deformation of nanotubes. Similar synchronized deformation is often observed even at the interlayer space between inner and outer nanotubes in concentric DWNTs.

It has been expected that the A-DWNT would have an ideal interaction between an already formed outer nanotube and a thermally transforming inner nanotube from fullerene molecules, because the encapsulated fullerene molecules change into the inner nanotube using the outer one as a template. It is quite reasonable to assume that the diameter of the inner tube depends on the outer one. However, we could not find an expected relationship in the chiral angle between the nested nanotubes. Saito *et al.* have calculated the van der Waals interaction for DWNTs with various chiral index pairs and found that the stable chiral index pair does not depend on chirality of nanotubes but the interlayer distance [13]. It is essentially impossible for the two nested tubes in various DWNTs to exhibit a complete graphitic stacking all over their interfaces. Even if a DWNT has a quite strong interaction between two layers, such a commensurate stacking can be achieved only in a limited area. After all, the morphology of the DWNT is strongly governed by the competition between the van der Waals force and the elastic force: the van der Waals force tends to produce the commensurate stacking and leads to local deformation of a nanotube, while the elastic force prefers to keep a concentric arrangement with a constant interlayer spacing of two nested nanotubes. In good contrast to carbon DWNTs, the interlayer interaction in BN DWNT is believed to be much effective to stack BN layers with an atomic correlation. It has been often reported that zigzag type (with zero chiral angle) is dominant in multiwall BN nanotubes, which is energetically preferable [14]. This is most probably attributed to the more robust interaction of adjacent BN layers, which necessitates a (partially) commensurate stacking in multiwall BN nanotubes.

It has been both experimentally and theoretically demonstrated that adjacent SWNTs in a bundle can merge to

form a larger tube by electron irradiation at elevated temperatures [15,16]. In our experiments, elastic deformations of nanotubes have been frequently observed to achieve a local commensurate stacking. This can also support a theoretical suggestion by Kawai *et al.* [16], in which the coalescence of two nanotubes with different chirality can start at the local region where hexagonal structures in graphene layers match commensurately. Further, it is quite intriguing to investigate electronic properties of eccentric DWNTs and circumscribed nanotubes with the local atomic correlation as well as concentric DWNTs, as the theoretical calculations have predicted for some adjacent commensurate nanotubes with specific chiral index [1–3,17].

We acknowledge T. Nakanishi for fruitful comments. This work is supported by the NEDO Nano-Carbon Technology project. A. H. is grateful to the Japan Society for the Promotion of Science for Young Scientists for financial support.

*To whom correspondence should be addressed.

E-mail: hashimoto-aya@aist.go.jp

- [1] D.-H. Kim, H.-S. Sim, and K. J. Chang, *Phys. Rev. B* **64**, 115409 (2001).
- [2] S. Sanvito, Y.-K. Kwon, D. Tománek, and C. J. Lambert, *Phys. Rev. Lett.* **84**, 1974 (2000).
- [3] R. Saito, G. Dresselhaus, and M. S. Dresselhaus, *J. Appl. Phys.* **73**, 494 (1993).
- [4] R. Pfeiffer, H. Kuzmany, Ch. Kramberger, Ch. Schaman, T. Pichler, H. Kataura, Y. Achiba, J. Kürti, and V. Zólyomi, *Phys. Rev. Lett.* **90**, 225501 (2003).
- [5] M. Abe, H. Kataura, H. Kira, T. Kodama, S. Suzuki, Y. Achiba, K. Kato, M. Takata, A. Fujiwara, K. Matsuda, and Y. Maniwa, *Phys. Rev. B* **68**, 041405 (2003).
- [6] M. Kociak, K. Hirahara, K. Suenaga, and S. Iijima, *Eur. Phys. J. B* **32**, 457 (2003).
- [7] J. M. Zuo, I. Vartanyants, M. Gao, R. Zhang, and L. A. Nagahara, *Science* **300**, 1419 (2003).
- [8] S. Bandow, M. Takizawa, K. Hirahara, M. Yudasaka, and S. Iijima, *Chem. Phys. Lett.* **337**, 48 (2001).
- [9] T. Sugai, T. Okazaki, H. Yoshida, and H. Shinohara, *New J. Phys.* **6**, 21 (2004).
- [10] A. Hashimoto, K. Suenaga, A. Gloter, K. Urita, and S. Iijima, *Nature (London)* **430**, 870 (2004).
- [11] Ph. Lambin and A. A. Lucas, *Phys. Rev. B* **56**, 3571 (1997).
- [12] C. Qin and L.-M. Peng, *Phys. Rev. B* **65**, 155431 (2002).
- [13] R. Saito, R. Matsuo, T. Kimura, G. Dresselhaus, and M. S. Dresselhaus, *Chem. Phys. Lett.* **348**, 187 (2001).
- [14] D. Golberg, Y. Bando, K. Kurashima, and T. Sato, *Solid State Commun.* **116**, 1 (2000).
- [15] M. Terrones, H. Terrones, F. Banhart, J.-C. Charlier, and P. M. Ajayan, *Science* **288**, 1226 (2000).
- [16] T. Kawai, Y. Miyamoto, O. Sugino, and Y. Koga, *Phys. Rev. Lett.* **89**, 085901 (2002).
- [17] T. Nakanishi and T. Ando, *J. Phys. Soc. Jpn.* **70**, 1647 (2001).